THE JOURNAL OF PHYSICAL CHEMISTRY B

Article

pubs.acs.org/JPCB

Probing Ternary Complex Equilibria of Crown Ether Ligands by Time-Resolved Fluorescence Spectroscopy

M. Thomas Morgan, S. Sumalekshmy, Mysha Sarwar, Hillary Beck, Stephen Crooke, and Christoph J. Fahrni*

School of Chemistry and Biochemistry and Petit Institute for Bioengineering and Bioscience, Georgia Institute of Technology, 901 Atlantic Drive, Atlanta, Georgia 30332, United States

Supporting Information

ABSTRACT: Ternary complex formation with solvent molecules and other adventitious ligands may compromise the performance of metal-ion-selective fluorescent probes. As Ca(II) can accommodate more than 6 donors in the first coordination sphere, commonly used crown ether ligands are prone to ternary complex formation with this cation. The steric strain imposed by auxiliary ligands, however, may result in an ensemble of rapidly equilibrating coordination species with varying degrees of interaction between the cation and the specific donor atoms mediating the fluorescence response, thus diminishing the change in fluorescence properties upon Ca(II) binding. To explore the influence of ligand architecture on these equilibria, we tethered two structurally distinct aza-15-crown-5 ligands to pyrazoline fluorophores as reporters. Due to ultrafast photoinduced electron-transfer (PET) quenching of the fluorophore by the ligand moiety, the fluorescence decay profile directly reflects the species composition in the ground state. By adjusting the PET driving force through electronic tuning of the pyrazoline fluorophores, we were able to differentiate between species with only subtle variations in PET donor abilities. Concluding from a global analysis of the corresponding fluorescence decay profiles, the coordination species composition was indeed strongly dependent on the ligand architecture. Altogether, the combination of time-resolved fluorescence spectroscopy with selective tuning of the PET driving force represents an effective analytical tool to study dynamic coordination equilibria and thus to optimize ligand architectures for the design of high-contrast cation-responsive fluorescence switches.

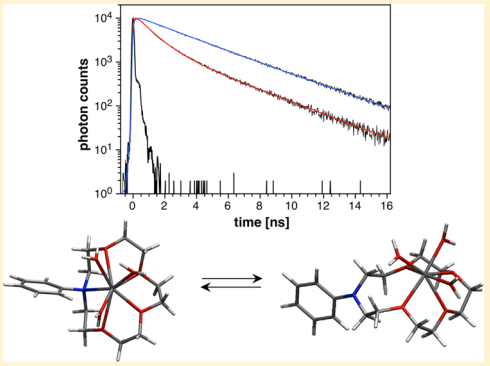

1. INTRODUCTION

Macrocyclic ligands, particularly aza-substituted crown and thiocrown ethers, are commonly utilized in the design of cation-selective fluorescent probes responding with either a spectral shift or enhancement in fluorescence emission.[1,2] If an *N*-aryl azacrown moiety serves as the electron-donor in fluorophore platforms with donor−acceptor (D−A) architecture, the degree of excited-state intramolecular charge transfer (ICT) decreases upon metal cation binding to produce a hypsochromic shift in the fluorescence emission. Alternatively, if the crown ether-based electron donor is electronically decoupled from the fluorophore π-system, it can quench fluorescence via photoinduced electron transfer (PET), yielding an increased emission intensity upon coordination of the cation via suppression of PET. The overall fluorescence contrast, defined as the ratio of emission intensities between the metal-bound and free forms, is dependent on the change in PET driving force, which in turn is governed by the increase in donor potential upon metal binding.[3] Thus, the fluorescence contrast and final quantum yield are dependent on the ability of the metal cation to reduce the PET donor strength. In previous work with *N*-aryl thiazacrown-based Cu(I)-responsive fluorescent probes, in which the arylamine moiety serves as the PET donor, we observed that the fluorescence contrast ratios and quantum yields are significantly compromised by formation of ternary complexes with solvent molecules, which allow for dissociation of the Cu(I)−N bond and thus significant residual PET.[4] We suspected that such effects are not confined to Cu(I)−thiazacrown systems but might extend to other ligands and metal ions as well. In fact, Freidzon et al. had previously conducted computational studies of ternary complex formation in the Ca(II)-*N*-phenylaza-15-crown-5 system in an effort to explain a long wavelength shoulder observed in the absorption spectrum of Ca(II) responsive styryl dyes containing this ligand motif.[5−7] Furthermore, X-ray structural analysis of the Ca(II)-*N*-phenylaza-15-crown-5 complex revealed the presence of three water molecules in the first coordination sphere.[8] As illustrated with Scheme 1A, ternary complex formation with solvent molecules may increase the steric strain to push the equilibrium toward coordination species with weakened Ca−N interaction,[6] thus increasing the electron donating ability of the aniline moiety. In the case of styryl dyes, this results in

Special Issue: Spectroscopy of Nano- and Biomaterials Symposium

Received: July 31, 2014
Revised: September 26, 2014
Published: October 14, 2014

   dx.doi.org/10.1021/jp5077406 | J. Phys. Chem. B 2014, 118, 14196−14202

Scheme 1

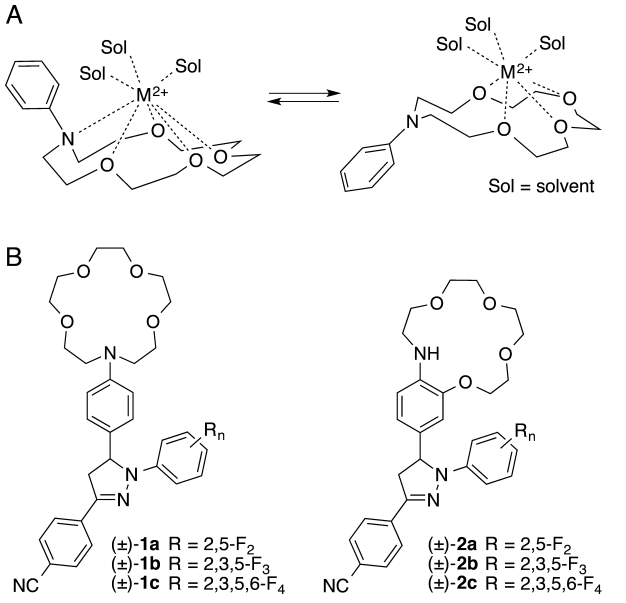

increased ICT and thus a longer absorption and emission wavelength. As the equilibration between different coordination species likely occurs with rapid kinetics, individual coordination species may not be distinguishable by solution NMR methods.[4,9] Therefore, we decided to study this system by picosecond-resolved fluorescence spectroscopy as an extension of our previous work on the design of Cu(I)-responsive fluorescent probes.[4,10−13]

For this purpose, we combined the *N*-phenylaza-15-crown-5 ligand, as well as a modified version with the aryl ring fused to the ligand backbone, with electronically decoupled pyrazoline fluorophores as PET-sensitive fluorescence reporters (Scheme 1B). Compared to probe **1**, the ring-fused ligand of **2** was expected to reduce steric strain between the ortho-hydrogen atoms of the aniline ring and the ligand backbone in the ternary complex,[9,14] thus suppressing dissociation of the metal−nitrogen bond for improved contrast and quantum yield.[15]

Given the different donor strengths for PET quenching, each species is expected to exhibit a characteristic fluorescence lifetime, thus yielding a multiexponential decay profile if more than one coordination species is present in solution. Due to the correlative relationship between the pre-exponential terms and fluorescence lifetimes, least-squares fitting of multiexponential decay data can yield more than a single solution with satisfactory statistics.[16] For this reason, we thought to measure the fluorescence decay profiles at three different PET driving forces and perform a global analysis based on a single set of pre-exponential components reflecting the fractional contribution of each species. Taking advantage of the electronic tunability of 1,3,5-triarylpyrazoline fluorophores,[3,17] we synthesized a set of three derivatives for each ligand, **1a−c** and **2a−c**, respectively, with an increasing number of fluoro-substituents on the 1-aryl ring (Scheme 1B, Table 1). As previously demonstrated, the increasing electron withdrawing character of the 1-aryl ring enhances the excited-state energy while leaving the fluorophore acceptor potential mostly unchanged.[3,17] As a consequence, the PET driving force steadily increases with the number of fluoro substituents. Although the radical cation formed by PET may promote a significant reorganization of the metal−ligand interaction and even lead to metal ejection,[18−20] PET quenching of the electronically decoupled fluorophore precedes subsequent rearrangements, and therefore the fluorescence decay profile is a direct reflection of the ensemble composition in the ground state at the time of excitation. Furthermore, unlike a directly coupled ICT-based fluorescence reporter, the attachment of the pyrazoline fluorophore via an sp^3-hybridized carbon is not expected to substantially perturb the donor strength of the arylamine nitrogen compared to the unsubstituted ligand.

2. EXPERIMENTAL METHODS

Synthesis. Procedures for the synthesis of compounds **1a−c**, **2a−c**, and all intermediates are provided in the Supporting Information.

Steady-State Absorption and Fluorescence Spectroscopy. UV−vis absorption spectra were acquired at 25 °C with a Varian Cary Bio50 spectrophotometer with constant temperature accessory. Emission spectra were recorded with a PTI fluorometer and corrected for the spectral response of the detection system and the spectral irradiance of the excitation source (through a calibrated photodiode). To convert the emission spectra to wavenumber scale, the measured emission intensities were corrected by multiplication with λ^2.[21] All measurements were conducted in a quartz cuvette with 1 cm path length and a cell volume of 3.0 mL with HPLC grade acetonitrile as the solvent. Quantum yields were determined in air-equilibrated solutions using norharmane in 0.1 N H_2SO_4 as fluorescence standard (Φ_f = 0.58).[22]

Picosecond Time-Resolved Fluorescence Spectroscopy. The fluorescence decay profiles were acquired in air-equilibrated HPLC grade acetonitrile in a 1 cm path length quartz cuvette at a fluorophore concentration of 5 μM using a single photon counting spectrometer (Edinburgh Instruments, LifeSpec Series) equipped with a pulsed laser diode as the excitation source (372 nm, FMHM = 80 ps, 20 MHz repetition rate, 1024 channel resolution). The wavelength of the emission monochromator was adjusted to the emission maximum of the respective fluorophore. The decay data were analyzed by nonlinear least-squares fitting with deconvolution of the instrument response function using the DecayFit software package.[23]

Cyclic Voltammetry. The donor and acceptor potentials of each probe were determined in deoxygenated acetonitrile containing 0.1 M Bu_4NPF_6 as the electrolyte using a CH-Instruments potentiostat equipped with a single compartment cell with a glassy carbon working electrode, a Pt counter electrode, and a nonaqueous $Ag/AgNO_3$ reference electrode (10 mM). The measured potentials were referenced to ferrocene as external standard. All measurements were performed at a scan rate of 100 mV s^{-1}.

Determination of Stability Constants. Titrations were carried out in acetonitrile at a probe concentration of 5 μM by addition of $Ca(ClO_4)_2 \cdot 4H_2O$ up to a total concentration of 10 mM. After addition of each aliquot, the solution was equilibrated for 5 min and a fluorescence spectrum was acquired over the entire emission range. The data were analyzed by nonlinear least-squares fitting based on equation S5 as described in the Supporting Information.

3. RESULTS AND DISCUSSION

Synthesis. The two sets of fluorescent probes **1** and **2** were synthesized from the corresponding aldehyde precursors **3** and

dx.doi.org/10.1021/jp5077406 | J. Phys. Chem. B 2014, 118, 14196−14202

Scheme 2. Synthesis of Pyrazoline Derivatives 1a–c (A) and 2a–c (B)

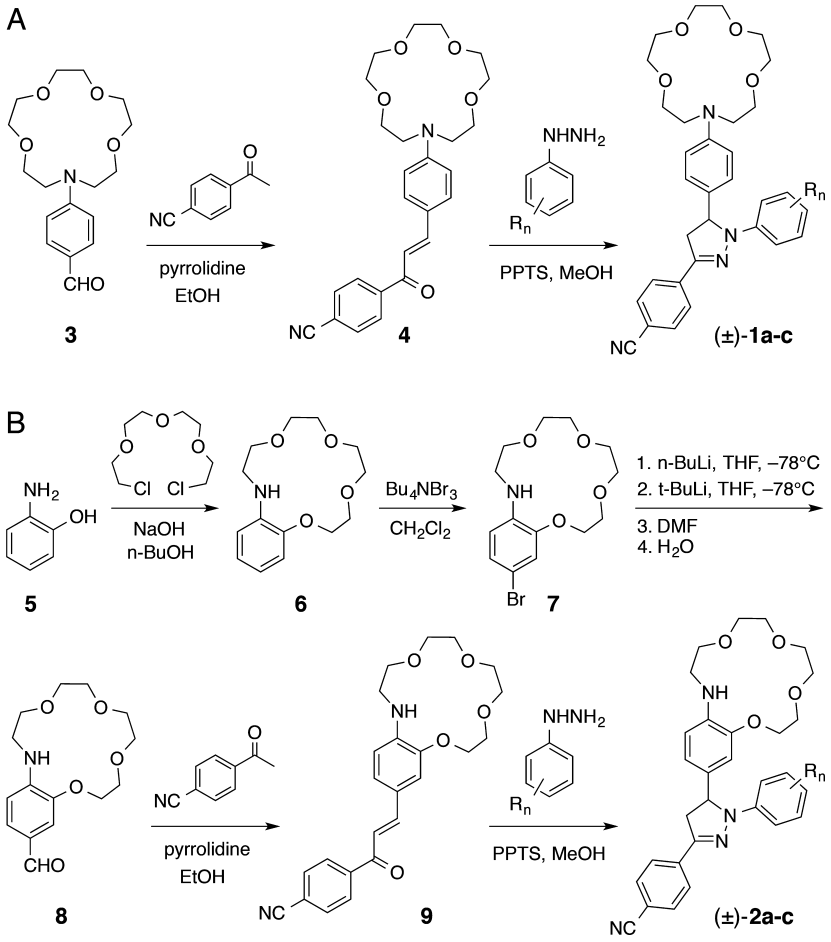

6, respectively, by aldol condensation with *para*-cyano acetophenone followed by cyclization of the chalcone intermediates with the respective fluoro-substituted arylhydrazines (Scheme 2). Aldehyde **3** was obtained through Vilsmeier formylation of commercially available *N*-phenylaza-15-crown-5,[24] whereas **8** was accessed through lithium halogen exchange of bromide **7** followed by quenching with dimethylformamide. Ligand **6** was synthesized from 2-aminophenol by cyclization with tetraethylene glycol dichloride according to a literature procedure,[9] and converted to **7** by bromination with tetrabutylammonium tribromide. Each probe was isolated by column chromatography and further purified by recrystallization from MTBE–cyclohexane.

Steady-State Absorption and Emission Spectroscopy. As the stability of crown ether complexes is significantly reduced in protic compared to nonprotic solvents, all complexation studies were conducted in acetonitrile. We selected Ca(II) as the metal cation to probe ternary complex formation, as it has been frequently used in complexation studies of *N*-phenylaza-15-crown-5 derivatives.[8,24–32] Ca(II) was supplied as $CaClO_4{\cdot}4H_2O$, yielding four water molecules per Ca(II) center, a number that satisfies the stoichiometry of ternary complexes according to experimental and computational studies.[6–8] The pertinent photophysical properties of the pyrazoline probes **1** and **2** are compiled in Table 1. Due to the low quantum yield of the free probes, the emission maxima were determined in the presence of a large excess of $Ca(ClO_4)_2{\cdot}4H_2O$. The PET driving force for each derivative was estimated on the basis of the Rehm–Weller formalism[33] using the experimentally determined ground-state donor and acceptor potentials (Supporting Information).

Table 1. Photophysical Data of Pyrazoline Derivatives 1a–c and 2a–c in Acetonitrile at 298 K

compd	R	abs λ_{max}/nm	em λ_{max}/nm[a]	ΔE_{00}/eV[b]	ΔG_{et}/eV[c]	Φ_F[d]
1a	2,5-F_2	377	489	2.90	−0.27	0.68
1b	2,3,5-F_3	371	475	2.97	−0.35	0.42
1c	2,3,5,6-F_4	357	450	3.09	−0.42	0.32
2a	2,5-F_2	377	489	2.90	−0.35	0.71
2b	2,3,5-F_3	370	471	2.98	−0.45	0.73
2c	2,3,5,6-F_4	354	451	3.11	−0.51	0.79

[a]Measured in the presence of 0.1 M $Ca(ClO_4)_2{\cdot}4H_2O$. [b]Zero–zero transition energy; estimated as $\bar{\nu}_{00} \approx 1/2(\bar{\nu}_{abs}^{max} + \bar{\nu}_{em}^{max})$.[34] [c]Photoinduced electron-transfer free energy estimated on the basis of the Rehm–Weller formalism[33] using experimental ground-state donor and acceptor potentials (Supporting Information). [d]Apparent fluorescence quantum yield; norharmane in 0.1 N H_2SO_4 as reference (Φ_f = 0.58).[22]

Consistent with previous observations on 1,3,5-triarylpyrazoline fluorophores, the absorption and emission bands of all derivatives are broad and unstructured, indicating a lowest excited state with charge-transfer character (Figure 1).[4,27,35] With increasing number of fluoro-substituents on the 1-aryl ring, the absorption and emission maxima are shifted to higher energy while maintaining similar Stokes shifts (Figure 1),[3,17]

dx.doi.org/10.1021/jp5077406 | J. Phys. Chem. B 2014, 118, 14196–14202

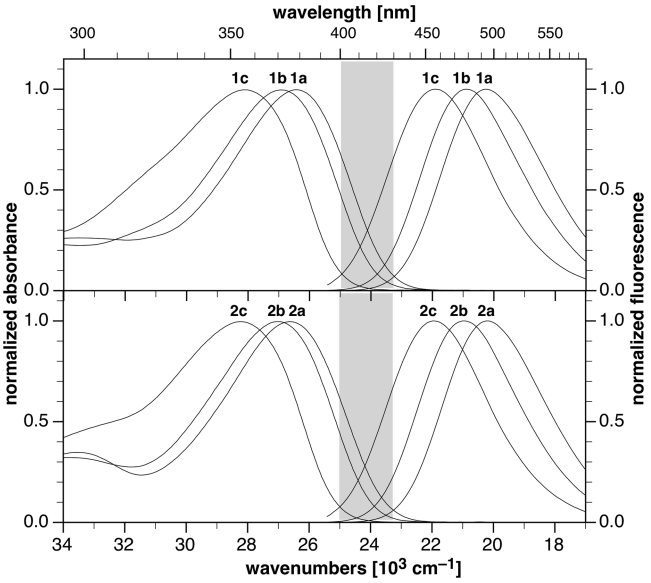

Figure 1. Normalized absorption (left traces) and emission spectra (right traces) of pyrazoline derivatives **1a**–**c** and **2a**–**c** in acetonitrile in the presence of 0.1 M $Ca(ClO_4)_2{\cdot}4H_2O$ at 298 K. The shaded area indicates the tunable range of the 0–0 transition energy to the lowest excited state.

and consequently the zero–zero excited-state energies ΔE_{00} increase from 2.90 to 3.11 eV with approximately 0.1 eV increments (Table 1). Because the crown ether moiety is electronically decoupled from the fluorophore π-system, both sets of probes exhibit very similar absorption and emission trends; however, the PET driving force differs by approximately 80–100 mV between derivatives with identical numbers of fluoro substituents. This difference can be attributed to the lower donor potential of the crown ether moiety in series **2**, which features an additional oxygen π-donor for improved stabilization of the radical cation. Despite the higher PET driving force, the apparent fluorescence quantum yields of the Ca(II)-saturated probes consistently remain above 70% in the **2** series but decrease from 0.68 to 0.32 for **1**, indicating an incomplete fluorescence recovery.

Proton NMR Analysis. In previous work with Cu(I)–thiazacrown systems,[4] including the direct thio-analogue of *N*-phenylaza-15-crown-5,[36] we observed a single set of NMR resonances at all Cu(I)–ligand ratios, indicating that the binary complex, free ligand, and any ternary complexes present all equilibrate rapidly on the NMR time scale. To determine whether this is also the case for the Ca(II)–*N*-phenylaza-15-crown-5 system, we recorded ^{1}H NMR spectra of this ligand in the absence and presence of 0.1 M $Ca(ClO_4)_2{\cdot}4H_2O$. As shown in Figure 2, addition of excess Ca(II) to a solution of the ligand in CD_3CN resulted in substantial deshielding of all aryl protons; however, only a single resonance for each set of equivalent protons in the ligand was observed, indicating that all coordination species present equilibrate too rapidly to be distinguished by proton NMR.

Coordination Equilibria with Ca(II). To determine the apparent binding affinity and complex stoichiometry of the fluorescent probes, we performed a series of fluorescence titrations with $Ca(ClO_4)_2{\cdot}4H_2O$ in acetonitrile. Because the metal ion binding sites are electronically decoupled from the fluorophore moieties, we anticipated only minor affinity variations across derivatives of the same series. For this reason

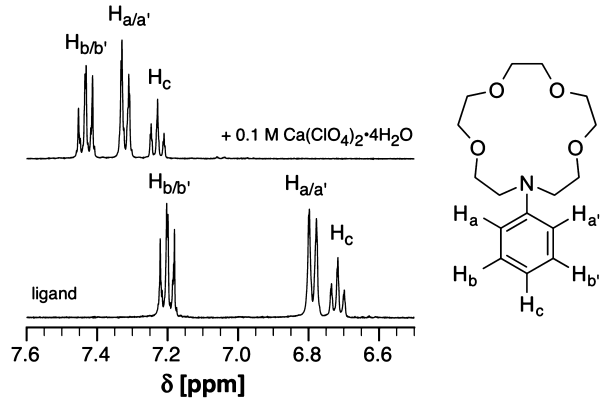

Figure 2. Aromatic region of the ^{1}H NMR spectrum of *N*-phenylaza-15-crown-5 (25 mM) in the presence (top trace) and absence (bottom trace) of 0.1 M $Ca(ClO_4)_2{\cdot}4H_2O$ in acetonitrile-d_3 at 298 K.

we restricted the Ca(II) binding affinity studies to derivatives **1c** and **2c** as representative examples. Both compounds displayed negligible fluorescence emission in their free form but responded with strong fluorescence enhancements upon saturation with Ca(II) (Figure 3). Due to the low quantum yield of the free forms, it was not possible to extract reliable fluorescence enhancement factors; nevertheless, the data indicate that the fluorescence contrast exceeds 1:1000 for both probes. Given the rapid equilibration between different

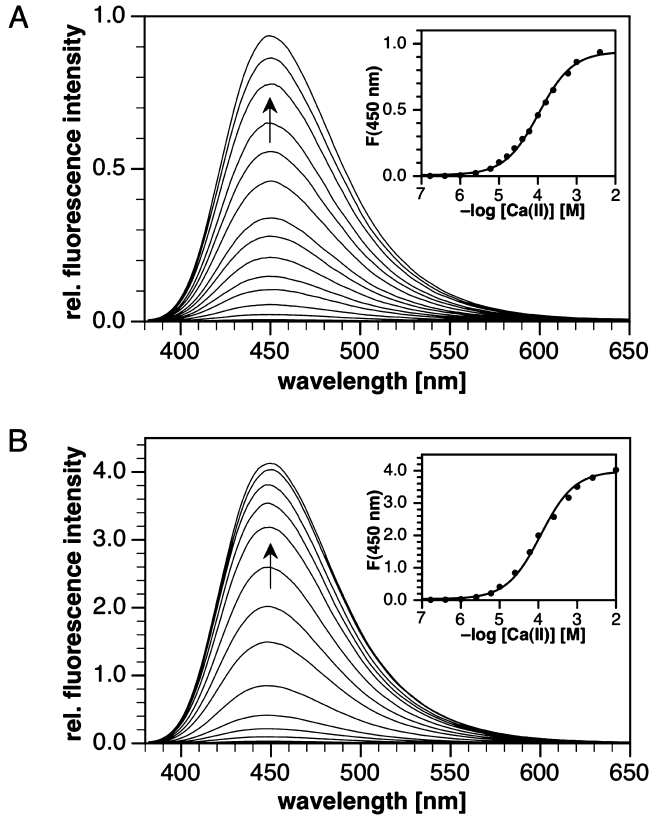

Figure 3. Fluorescence emission spectra of pyrazoline derivative **1c** (A) and **2c** (B) in acetonitrile as a function of the total concentration of $Ca(ClO_4)_2{\cdot}4H_2O$. The inset shows the fluorescence intensity at 450 nm and the corresponding Ca(II) concentrations for each trace, as well as the curve-fit for a binding isotherm with 1:1 metal-probe stoichiometry using equation S5 (Supporting Information).

dx.doi.org/10.1021/jp5077406 | *J. Phys. Chem. B* 2014, 118, 14196–14202

Table 2. Time-Resolved Fluorescence Decay Data for Pyrazoline Derivatives 1a−c and 2a-c and Reference Compounds 3a−c in Acetonitrile Containing 0.1 M $Ca(ClO_4)_2 \cdot 4H_2O$ at 25 °C

compd	R	τ /ns	χ^2 [a]
1a	2,5-F_2	3.22	1.578
		4.06 (0.26); 2.89 (0.74)[b]	1.212
1b	2,3,5-F_3	3.61 (0.26); 1.88 (0.74)[b]	1.104
1c	2,3,5,6-F_4	2.99 (0.26); 0.91 (0.74)[b]	1.220
2a	2,5-F_2	3.95	1.318
2b	2,3,5-F_3	3.78	1.166
2c	2,3,5,6-F_4	3.01	2.412
		3.19 (0.88); 1.62 (0.12)[c]	1.408
3a	2,5-F_2	3.99[d]	
3b	2,3,5-F_3	3.74	1.248
3c	2,3,5,6-F_4	3.09[d]	

[a]Goodness of fit parameter. [b]Global least-squares fit with biexponential decay model (global χ^2 = 1.179). [c]Least-squares fit with unconstrained biexponential decay model. [d]Data from ref 3.

coordination species, the steady-state fluorescence data reflect an ensemble-averaged response of the probes toward Ca(II) binding. Nonlinear least-squares fitting of the fluorescence intensity at 450 nm as a function of Ca(II) concentrations fit well to an equilibrium model with 1:1 metal−ligand stoichiometry and yielded the apparent stability constants of log K = 3.98 ± 0.02 and 3.94 ± 0.04 for derivatives **1c** and **2c**, respectively (Supporting Information). These values are comparable to the Ca(II) stability constants of other fluorescent probes featuring the same parent ligand *N*-phenylaza-15-crown-5.[8,25,27] In the presence of 1% (0.56 M) additional water, the apparent stability constant of **1c** decreased to log K = 2.12 ± 0.02, and even further to log K = 1.71 ± 0.02 in the case of derivative **2c** (Figures S1 and S2, Supporting Information). The somewhat lower affinity of **2c** is possibly due to additional stabilization of the N−H functionality in the free ligand through hydrogen bonding with water molecules, which must be reorganized upon binding of Ca(II).

Time-Resolved Fluorescence Decay Data. The lower recovery quantum yields observed for **1a−c** compared to **2a−c** upon saturation with Ca(II) is indicative of a weakened interaction between the metal ion and the aniline nitrogen donor, possibly involving the formation of various equilibrating coordination species. To investigate whether multiple coordination species contribute to the observed fluorescence recovery, we performed picosecond time-resolved fluorescence decay measurements. Depending on the interaction strength between the metal ion and PET donor, the different coordination species are expected to exhibit distinct fluorescence decay lifetimes. Each probe was dissolved in acetonitrile containing 0.1 M $Ca(ClO_4)_2 \cdot 4H_2O$, a concentration at which complex formation is complete by >99.9% based on the measured Ca(II) stability constants. All compounds were excited at 372 nm with a pulsed laser, and the decay signal was collected at the maximum emission wavelength by single photon counting. The fluorescence lifetimes were determined from nonlinear least-squares fitting of the decay profiles with mono- or biexponential decay models (Table 2). We also include in Table 2 data from reference compounds **3a−c** carrying a simple phenyl ring in the 5-position in lieu of the arylazacrown moiety to gauge the intrinsic lifetime of the fluorophore in the absence of PET.[3]

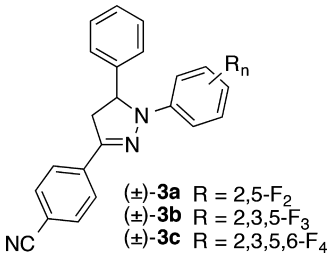

As evident from the multiexponential fluorescence decay profiles displayed in Figure 4A, the pyrazoline derivatives **1a−c** produce more than a single coordination species with Ca(II). Although the time trace of **1a** can be fit to a single lifetime of 3.22 ns, the quality of the fit improves significantly with a biexponential decay model (Table 2). Because the metal binding site is electronically decoupled from the fluorophore π-system, the species composition is expected to remain uniform across all three derivatives. In agreement with this notion, it was possible to extract a single pair of pre-exponential factors through global least-squares curve fitting[23] of the three decay profiles using a biexponential decay model (Table 2). Despite the fitting constraints, each decay profile fit to the same pair of pre-exponential factors with an excellent global χ^2 value of 1.179 (Table 2). The longer lifetime component, which contributes 26% to the decay signal, matches within ~0.1 ns the lifetime of the respective reference compounds **3a−c**, indicating effective inhibition of PET and complete fluores-

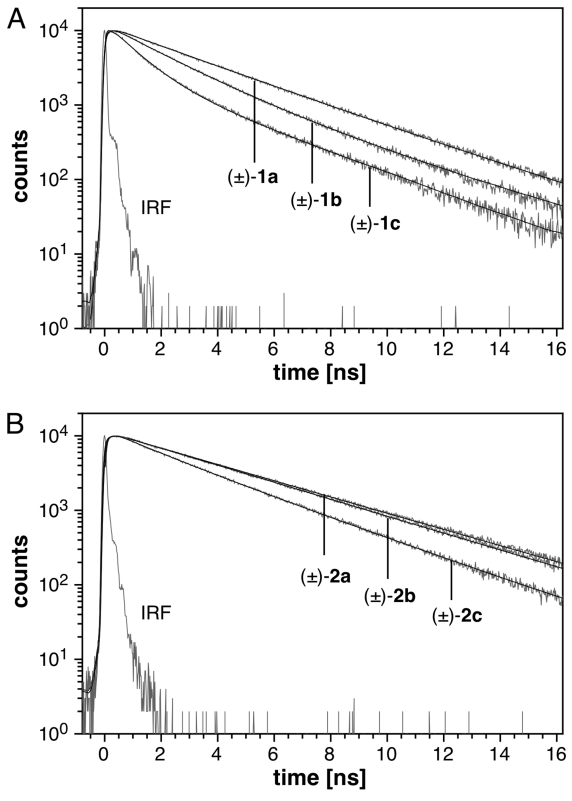

Figure 4. Fluorescence decay profiles of pyrazoline derivatives **1a−c** (A) and **2a−c** (B) in acetonitrile in the presence of 0.1 M $Ca(ClO_4)_2 \cdot 4H_2O$. Each sample was excited at 372 nm (80 ps fwhm), and the decay signal was detected at the maximum emission wavelength by single photon counting. Nonlinear least-squares fitted traces are shown as solid lines (IRF = instrument response function; see Table 2 for curve fitting data).

dx.doi.org/10.1021/jp5077406 | J. Phys. Chem. B 2014, 118, 14196−14202

cence recovery. In contrast, the lifetime of the more prevalent component, which contributes 74% to the decay signal, is consistently shorter and decreases significantly from to 2.89 to 0.91 ns with increasing PET driving force (Table 2). Consistent with the observed decrease of the ensemble-averaged quantum yields (Table 1), the differences in fluorescence decay lifetimes between the two coordination species is more pronounced at higher PET driving force.

To test whether the species with shorter fluorescence lifetimes might arise from direct Ca(II) interactions with the pyrazoline fluorophore, we measured the decay profile under acidic conditions in the presence of 0.1 M $Ca(ClO_4)_2 \cdot 4H_2O$ and 1 mM methanesulfonic acid. Concluding from the monoexponential decay (Figure S5B, Supporting Information) and fluorescence lifetime of 3.13 ns, which agrees well with that of the unquenched reference compound **3c** (Table 1), the emission is completely restored through protonation of the aniline nitrogen and thus Ca(II)−pyrazoline interactions do not appear to constitute a significant nonradiative deactivation pathway. Hence, the fluorescence lifetime data are consistent with the presence of a coordination species in which the metal−ligand donor interaction is weakened to alleviate steric strain imposed by the auxiliary solvent ligands. Interestingly, the fluorescence decay profile of **1c** acquired under anhydrous conditions using rigorously dried $Ca(ClO_4)_2$ remain unchanged (Figure S5C, Supporting Information), suggesting that acetonitrile rather than water is engaged in ternary complex formation.

In contrast to **1a−c**, the fluorescence decay profiles of **2a−c** appear to involve only a single component (Figure 4B). In the case of **2a** and **2b**, deconvolution of the decay profiles with a monoexponential decay model produced excellent least-squares curve fits with lifetimes closely matching those of the reference compounds **3a** and **3b**, respectively. Although the decay profile of **2c** can be fit to a single lifetime of 3.01 ns matching reference compound **3c**, the fit is significantly improved with a biexponential decay model. However, unlike in the case of **1c**, the longer lifetime component is now the dominant contributor (88%), presumably indicating a strengthened Ca(II)−N interaction. At the same time, the shorter component (1.62 ns) is significantly longer-lived than that of **1c** (0.94 ns), despite the greater PET driving force of the free probe. This effect may be due to coordination of Ca(II) to the anisole oxygen of the PET donor even in the absence of a strong Ca−N interaction. Altogether, these data demonstrate that the modified azacrown ether ligand of probes **2a−c** engages Ca(II) more effectively in coordination to the actual electron donor moiety, which in turn results in more effective inhibition of PET quenching and full fluorescence recovery with a greater than 2-fold improvement in quantum yield for the tetrafluoro derivative **2c**.

4. CONCLUSIONS

Taking advantage of the tunable PET framework offered by 1,3,5-triarylpyrazoline fluorophores, we were able to specifically probe for rapidly equilibrating coordination species of two arylazacrown ether derivatives by picosecond time-resolved fluorescence spectroscopy. Similar to previous observations on Cu(I)-selective thiaza crowns,[4] the Ca(II)-solution chemistry of the *N*-phenylaza-15-crown-5 parent ligand of **1a−c** is characterized by the presence of at least two coordination species with distinct fluorescence decay lifetimes. As the difference in lifetimes not only is a function of the PET donor strength of each species but also depends on the contribution of the fluorophore to the PET driving force, the latter can be used as a tool to amplify lifetime differences and thus to differentiate between species with only subtle variations in PET donor abilities. As demonstrated for **1a−c**, the lifetime difference between the two components was small at the lowest PET driving force, resulting in an apparent monoexponential decay profile but substantially increased at more favorable driving forces to yield a biexponential decay with distinct lifetimes. In contrast, the fused-ring azacrown ligand of **2a** and **2b** produced uniform decay profiles with lifetimes that mirrored those of the reference compounds **3a** and **3b**, suggesting full fluorescence recovery upon saturation with Ca(II). Even the tetrafluoro derivative **2c**, which offers an initial PET driving force 90 mV higher than that of **1c**, achieved nearly complete fluorescence recovery with only 12% of a shorter-lived component in the decay lifetime. These differences are probably due to the more favorable ligand architecture of **2a−c** toward Ca(II) coordination, where the aryl ring is fully integrated into the ligand backbone and thus able to alleviate steric strain imposed by the ortho-hydrogens and solvent auxiliary ligands as in the case of **1a−c**. In summary, ternary complex formation with solvent molecules plays an important but often overlooked role in the design of high-contrast cation-selective fluorescent probes. In addition to the solvent, other adventitious ligands may contribute to ternary complex formation, e.g. if fluorescent probes are operating in a biological environment, as recently demonstrated by Bal and co-workers for the ZnAF family of zinc sensors.[37] The combination of time-resolved fluorescence spectroscopy with selective tuning of the PET driving force offers an effective analytical tool to probe ternary complex formation and thus to optimize ligand architectures for the design of high-contrast cation-responsive fluorescence switches.

■ ASSOCIATED CONTENT

Ⓢ Supporting Information

Synthetic procedures, ^{1}H-NMR and ^{13}C-NMR spectra, estimation of the photoinduced electron-transfer driving force (including a table of reduction potentials), data fitting for the determination of stability constants (including fluorescence titration plots), and fluorescence decay profiles. This material is available free of charge via the Internet at http://pubs.acs.org.

■ AUTHOR INFORMATION

Corresponding Author

*C. J. Fahrni. E-mail: fahrni@chemistry.gatech.edu.

Notes

The authors declare no competing financial interest.

■ ACKNOWLEDGMENTS

Financial support from the National Institutes of Health (R01GM067169), the National Science Foundation (Graduate Research Fellowship to S.C., Grant No. DGE-1148903), and the Georgia Tech Undergraduate Research Opportunities Program (President's Undergraduate Research Award to M.S.) is gratefully acknowledged.

■ REFERENCES

(1) de Silva, A. P.; Gunaratne, H. Q. N.; Gunnlaugsson, T.; Huxley, A. J. M.; McCoy, C. P.; Rademacher, J. T.; Rice, T. E. Signaling recognition events with fluorescent sensors and switches. *Chem. Rev.* **1997**, *97*, 1515.

(2) Valeur, B.; Leray, I. Design principles of fluorescent molecular sensors for cation recognition. *Coord. Chem. Rev.* **2000**, *205*, 3.
(3) Cody, J.; Mandal, S.; Yang, L. C.; Fahrni, C. J. Differential tuning of the electron transfer parameters in 1,3,5-triarylpyrazolines: A rational design approach for optimizing the contrast ratio of fluorescent probes. *J. Am. Chem. Soc.* **2008**, *130*, 13023.
(4) Chaudhry, A. F.; Verma, M.; Morgan, M. T.; Henary, M. M.; Siegel, N.; Hales, J. M.; Perry, J. W.; Fahrni, C. J. Kinetically controlled photoinduced electron transfer switching in Cu(I)-responsive fluorescent probes. *J. Am. Chem. Soc.* **2010**, *132*, 737.
(5) Ushakov, E. N.; Gromov, S. P.; Fedorova, O. A.; Alfimov, M. V. Crown-containing styryl dyes. 19. Complexation and cation-induced aggregation of chromogenic aza-15-crown-5 ether. *Russ. Chem. Bull.* **1997**, *46*, 463.
(6) Freidzon, A. Y.; Bagatur'yants, A. A.; Gromov, S. P.; Alfimov, M. V. Recoordination of a metal ion in the cavity of an arylazacrown ether: Model study of the conformations and microsolvation of calcium complexes of arylazacrown ethers. *Int. J. Quantum Chem.* **2004**, *100*, 617.
(7) Freidzon, A. Y.; Bagaturyants, A. A.; Gromov, S. P.; Alfimov, M. V. Recoordination of a metal ion in the cavity of a crown compound: a theoretical study - 2. Effect of the metal ion-solvent interaction on the conformations of calcium complexes of arylazacrown ethers. *Russ. Chem. Bull.* **2005**, *54*, 2042.
(8) Rurack, K.; Bricks, J. L.; Reck, G.; Radeglia, R.; Resch-Genger, U. Chalcone-analogue dyes emitting in the near-infrared (NIR): influence of donor-acceptor substitution and cation complexation on their spectroscopic properties and X-ray structure. *J. Phys. Chem. A* **2000**, *104*, 3087.
(9) Gromov, S. P.; Dmitrieva, S. N.; Vedernikov, A. I.; Kuz'mina, L. G.; Churakov, A. V.; Strelenko, Y. A.; Howard, J. A. K. Novel promising benzoazacrown ethers as a result of ring transformation of benzocrown ethers: Synthesis, structure, and complexation with Ca^{2+}. *Eur. J. Org. Chem.* **2003**, *2003*, 3189.
(10) Verma, M.; Chaudhry, A. F.; Morgan, M. T.; Fahrni, C. J. Electronically tuned 1,3,5-triarylpyrazolines as Cu(I)-selective fluorescent probes. *Org. Biomol. Chem.* **2010**, *8*, 363.
(11) Morgan, M. T.; Bagchi, P.; Fahrni, C. J. Designed to dissolve: Suppression of colloidal aggregation of Cu(I)-Selective fluorescent probes in aqueous buffer and in-gel detection of a metallochaperone. *J. Am. Chem. Soc.* **2011**, *133*, 15906.
(12) Morgan, M. T.; Bagchi, P.; Fahrni, C. J. High-contrast fluorescence sensing of aqueous Cu(I) with triarylpyrazoline probes: dissecting the roles of ligand donor strength and excited state proton transfer. *Dalton Trans.* **2013**, *42*, 3240.
(13) Fahrni, C. J. Synthetic fluorescent probes for monovalent copper. *Curr. Opin. Chem. Biol.* **2013**, *17*, 656.
(14) Gromov, S. P.; Dmitrieva, S. N.; Vedernikov, A. I.; Kurchavov, N. A.; Kuz'mina, L. G.; Strelenko, Y. A.; Alfimov, M. V.; Howard, J. A. K. N-Methylbenzoazacrown ethers with the nitrogen atom conjugated with the benzene ring: the improved synthesis and the reasons for the high stability of complexes with metal and ammonium cations. *J. Phys. Org. Chem.* **2009**, *22*, 823.
(15) Chaudhry, A. F.; Mandal, S.; Hardcastle, K. I.; Fahrni, C. J. High-contrast Cu(I)-selective fluorescent probes based on synergistic electronic and conformational switching. *Chem. Sci.* **2011**, *2*, 1016.
(16) Grinvald, A.; Steinberg, I. Z. On the analysis of fluorescence decay kinetics by the method of least-squares. *Anal. Biochem.* **1974**, *59*, 583.
(17) Verma, M.; Chaudhry, A. F.; Fahrni, C. J. Predicting the photoinduced electron transfer thermodynamics in polyfluorinated 1,3,5-triarylpyrazolines based on multiple linear free energy relationships. *Org. Biomol. Chem.* **2009**, *7*, 1536.
(18) Marcotte, N.; Plaza, P.; Lavabre, D.; Fery-Forgues, S.; Martin, M. M. Calcium photorelease from a symmetrical donor-acceptor-donor bis-crown-fluoroionophore evidenced by ultrafast absorption spectroscopy. *J. Phys. Chem. A* **2003**, *107*, 2394.
(19) Ley, C.; Lacombat, F.; Plaza, P.; Martin, M. M.; Leray, I.; Valeur, B. Femtosecond to subnanosecond multistep calcium photoejection from a crown ether-linked merocyanine. *ChemPhysChem* **2009**, *10*, 276.
(20) Rusalov, M. V.; Uzhinov, B. M.; Alfimov, M. V.; Gromov, S. P. Photoinduced recoordination of metal cations in complexes with chromogenic crown ethers. *Russ. Chem. Rev.* **2010**, *79*, 1099.
(21) Lakowicz, J. R. *Principles of Fluorescence Spectroscopy*; Springer: New York, 2006.
(22) Pardo, A.; Reyman, D.; Poyato, J. M. L.; Medina, F. Some beta-carboline derivatives as fluorescence standards. *J. Lumin.* **1992**, *51*, 269.
(23) *DecayFit* 1.4 - Fluorescence decay analysis software, FluoroTools, http://www.fluorotools.com, 2014.
(24) Oliveira, E.; Baptista, R. M. F.; Costa, S. P. G.; Raposo, M. M. M.; Lodeiro, C. Exploring the emissive properties of new azacrown compounds bearing aryl, furyl, or thienyl moieties: a special case of chelation enhancement of fluorescence upon interaction with Ca(II), Cu(II), or Ni(II). *Inorg. Chem.* **2010**, *49*, 10847.
(25) Kollmannsberger, M.; Rurack, K.; Resch-Genger, U.; Daub, J. Ultrafast charge transfer in amino-substituted boron dipyrromethene dyes and its inhibition by cation complexation: A new design concept for highly sensitive fluorescent probes. *J. Phys. Chem. A* **1998**, *102*, 10211.
(26) Delmond, S.; Letard, J.-F.; Lapouyade, R.; Mathevet, R.; Jonusauskas, G.; Rulliere, C. Cation-triggered photoinduced intramolecular charge transfer and fluorescence red-shift in fluorescence probes. *New J. Chem.* **1996**, *20*, 861.
(27) Rurack, K.; Bricks, J. L.; Schulz, B.; Maus, M.; Reck, G.; Resch-Genger, U. Substituted 1,5-diphenyl-3-benzothiazol-2-yl-2-pyrazolines: Synthesis, X-ray structure, photophysics, and cation complexation properties. *J. Phys. Chem. A* **2000**, *104*, 6171.
(28) Pearson, A. J.; Xiao, W. Fluorescent photoinduced electron transfer (PET) sensing molecules with *p*-phenylenediamine as electron donor. *J. Org. Chem.* **2003**, *68*, 5361.
(29) Kim, H. M.; Jeong, M.-Y.; Ahn, H. C.; Jeon, S.-J.; Cho, B. R. Two-photon sensor for metal ions derived from azacrown ether. *J. Org. Chem.* **2004**, *69*, 5749.
(30) Tang, W.-S.; Lu, X.-X.; Wong, K. M.-C.; Yam, V. W.-W. Synthesis, photophysics and binding studies of Pt(II) alkynyl terpyridine complexes with crown ether pendant. Potential luminescent sensors for metal ions. *J. Mater. Chem.* **2005**, *15*, 2714.
(31) Ho, M.-L.; Hwang, F.-M.; Chen, P.-N.; Hu, Y.-H.; Cheng, Y.-M.; Chen, K.-S.; Lee, G.-H.; Chi, Y.; Chou, P.-T. Design and synthesis of iridium(III) azacrown complex: application as a highly sensitive metal cation phosphorescence sensor. *Org. Biomol. Chem.* **2006**, *4*, 98.
(32) Qin, W.; Baruah, M.; Sliwa, M.; Van der Auweraer, M.; De Borggraeve, W. M.; Beljonne, D.; Van Averbeke, B.; Boens, N. Ratiometric, fluorescent BODIPY dye with aza crown ether functionality: synthesis, solvatochromism, and metal ion complex formation. *J. Phys. Chem. A* **2008**, *112*, 6104.
(33) Rehm, D.; Weller, A. Kinetics of fluorescence quenching by electron and hydrogen-atom transfer. *Isr. J. Chem.* **1970**, *8*, 259.
(34) Valeur, B.; Berberan-Santos, M. N. *Molecular Fluorescence: Principles and Applications*; Wiley-VCH: Weinheim, 2013.
(35) Fahrni, C. J.; Yang, L. C.; VanDerveer, D. G. Tuning the photoinduced electron-transfer thermodynamics in 1,3,5-triaryl-2-pyrazoline fluorophores: X-ray structures, photophysical characterization, computational analysis, and in vivo evaluation. *J. Am. Chem. Soc.* **2003**, *125*, 3799.
(36) Yang, L.; McRae, R.; Henary, M. M.; Patel, R.; Lai, B.; Vogt, S.; Fahrni, C. J. Imaging of the intracellular topography of copper with a fluorescent sensor and by synchrotron X-ray fluorescence microscopy. *Proc. Natl. Acad. Sci. U. S. A.* **2005**, *102*, 11179.
(37) Staszewska, A.; Kurowska, E.; Bal, W. Ternary complex formation and competition quench fluorescence of ZnAF family zinc sensors. *Metallomics* **2013**, *5*, 1483.